Towards Constraining Dark Sector e^+e^- Solutions to the Low Energy Excess at MicroBooNE

The MicroBooNE Collaboration*

June 13, 2024

1 Introduction

In recent years there has been a rapidly growing interest in "dark sector" physics that is accessible through neutrino experiments, motivated in part by long-standing experimental anomalies in short-baseline neutrino experiments. In many dark sector models, new unstable particles can be abundantly produced in neutrino-nucleus interactions. If these new states decay to photons or e^+e^- pairs with $\mathcal{O}(100)$ MeV energies [14, 13], their signature can mimic the excess of electron-like events observed by the MiniBooNE experiment [9]. While the origin of many of these theories was explaining the MiniBooNE excess, their popularity in the community has grown and they now represent a broad class of interesting models in their own right, outside of the short-baseline anomalies [8].

This note describes two ongoing efforts in MicroBooNE [6] investigating such dark sector models. In these models, active neutrinos from the Booster Neutrino Beam (BNB) upscatter to produce one or more heavy sterile neutrinos (or Dark Neutrinos), which subsequently decay into electron-positron pairs (e^+e^-), resulting in an excess that could be compatible with the MiniBooNE anomaly. While the dark sector may be quite rich phenomenologically, here a minimal $U(1)'$ gauge group is assumed with the dark neutrino being the only particle directly charged under this new group. The combination of neutrino mixing between active neutrinos and the dark neutrinos (the neutrino portal) as well as kinetic mixing between the dark gauge boson (Z') and our standard model photon (the vector portal) gives rise to the necessary phenomenology to explain the MiniBooNE excess. This process of upscattering to produce a visible e^+e^- signal is described pictorially in Fig. 1.

The differences and complementary of the two ongoing MicroBooNE dark-sector e^+e^- analyses, highlighting the dual-pronged approach taken, is shown below:

1. A **broad** analysis featuring both heavy ($m_{Z'} > m_h$) and light ($m_{Z'} << m_h$) dark gauge bosons, with one (3+1) or two (3+2) heavy sterile neutrinos (m_h and $m_{h'}$), targeting a wide class of dark sector models as described in A. Abdullahi *et al.* [1]. The analysis uses the Pandora pattern recognition reconstruction framework [7], and the BSM signal is provided by the open-source DarkNews [2] generator.

2. A **focused** light dark gauge boson ($m_{Z'} << m_h$) analysis targeting the specific model as introduced in E. Bertuzzo *et al.* [14]. This analysis uses the Wire-Cell reconstruction framework [5] and the signal is generated using the in-built dark neutrino generator included in GENIE version 3.2 [10].

In both models, for the e^+e^- pair to mimic the MiniBooNE anomaly the opening angle between the e^+e^- pair must be very small or the energy asymmetry between the produced e^+e^- pair must

*Email: microboone_info@fnal.gov

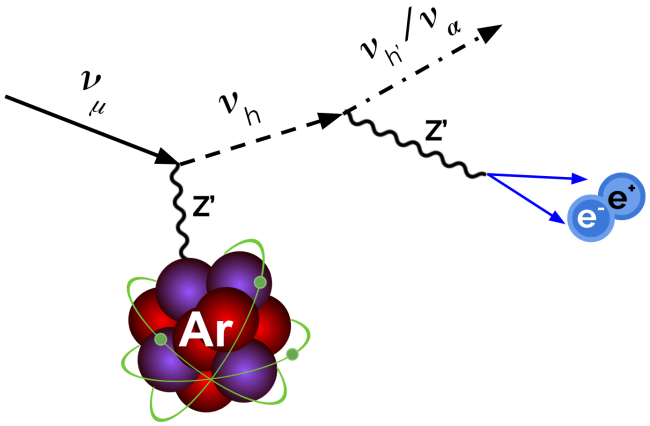

Figure 1: *A representative example of the upscattering dark neutrino models being searched for at MicroBooNE. An incoming muon-neutrino upscatters off an argon target, producing a heavy sterile neutrino (or dark neutrino, ν_h). Depending on the dark-sector content, the decay of the dark neutrino (ν_h) can be to a lighter dark-sector sterile neutrino ($\nu_{h'}$) or to an active neutrino (ν_α). Similarly, depending on the relative mass of the dark neutrino and the dark photon (Z'), the decay can be on or off-shell.*

be very large. While this is a requirement when considering dark sector explanations of the MiniBooNE signal, there is a wide array of model space where the opening angles between the e^+e^- may be small but non-negligible for a liquid argon time projection chamber (LArTPC) such as MicroBooNE. Figure 2 shows two example simulated dark sector e^+e^- event displays in MicroBooNE, one where the opening angle is small and thus the produced electromagnetic shower is indistinguishable from a true photon, and one where the opening angle is larger and the individual electron and positron are resolvable.

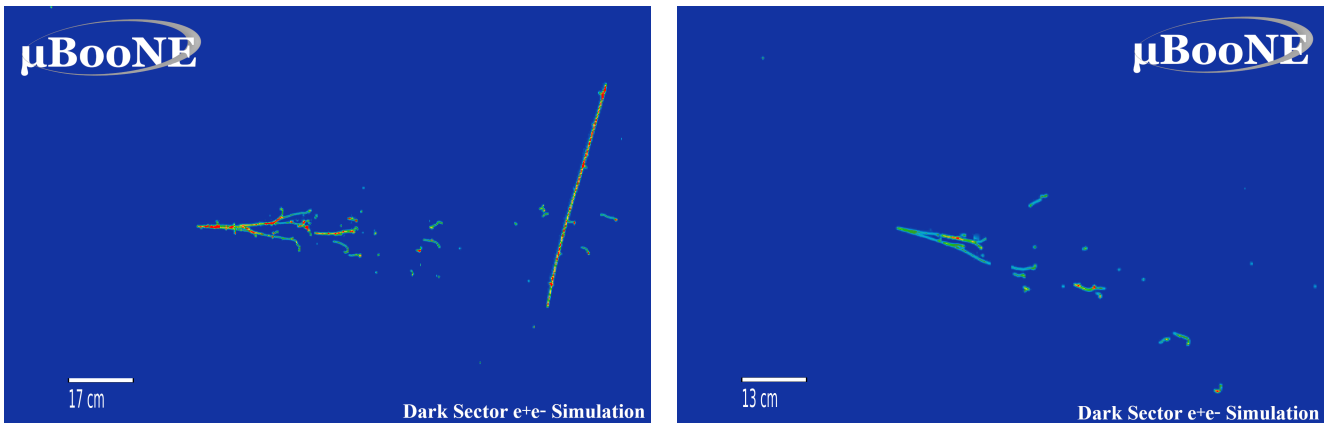

(a) ***(b)***

Figure 2: *Simulations of two Dark Sector e^+e^- pairs in MicroBooNE.* (a): *An example where the opening angle is small, and so the shower looks indistinguishable from a photon, e_{low} = 284.6 MeV, e_{high} = 332.8 MeV, e^+e^- opening angle* 5.58°. (b): *An example with a wider opening angle, allowing one to begin to resolve the individual components, e_{low} = 122.1 MeV, e_{high} = 188.1 MeV, e^+e^- opening angle* 16.7°.

2 A broad 3+1 and 3+2 dark sector search

While the minimal upscattering model contains just one heavy sterile (or dark) neutrino (ν_h), the so-called 3+1 model, the resulting requirement to decay back down to an active neutrino puts severe constraints on the allowed parameter space as this introduces a reduction in rate of $\mathcal{O}(|U_{\alpha 4}|^2)$. The inclusion of a second dark neutrino ($\nu_{h'}$) can bypass this restriction and instead replace it with an $\mathcal{O}(1)$ mixing between the two dark sector particles. The kinematics of the resulting event will be modified, with the key parameter being Δ, the dimensionless relative mass splitting between the two dark neutrinos, $\Delta \equiv (m_h - m_{h'})/m_{h'}$. When $\Delta >> 1$ the second sterile is very light compared to the primary sterile produced in the upscattering resulting in kinematics very similar to the reduced 3+1 scenario. When $\Delta < 1$, however, the second sterile plays an increasingly important role in the decay kinematics. If we compare to the Fig. 1, ν_h represents the heavier ν_5 and $\nu_{h'}$ is the lighter nu_4. A full description of the class of models, as well as its ability to describe the MiniBooNE anomaly, can be found in references [2, 12] and references therein. Depending on the mass of the dark gauge boson, the scattering can take place via either a coherent or incoherent process, although the focus of this analysis is the coherent scattering in which the signal is an e^+e^- pair only with no associated hadronic component. The wide range of model parameter space, including allowing for heavy $m_{Z'}$, gives rise to a very wide range of resulting e^+e^- kinematics including some with large e^+e^- opening angles.

This analysis targets this broad class of both 3+1 and 3+2 dark sector models, using 6.87×10^{20} protons-on-target of MicroBooNE's first three run periods. Unlike a pure photon search, in which we would be targeting single reconstructed shower topologies with no tracks (1s0t), e^+e^- pairs with wider opening angles or asymmetric energies can often be reconstructed as two-shower (2s0t) or one-shower and one-track (1s1t) events. This analysis targets all three of these primary expected topologies. Using the Pandora reconstruction framework, a series of four boosted decision trees (BDTs) are trained to reject various background categories while selecting dark-sector e^+e^- events. A cut is placed on these BDT scores to select a high efficiency, high purity sample of events. The resulting energy spectrum in simulation after these cuts can be found in Fig. 3 below. The total efficiency for selecting dark-sector e^+e^- events varies considerably across the model parameter space, but is typically of $\mathcal{O}(20-40\%)$. Figure 4 shows a representative efficiency as a function of true e^+e^- energy for a cocktail of dark sector model points.

The model space probed by this analysis is very large, featuring six key parameters in the 3+2 scenario that affect the resulting phenomenology. This includes the mass of the new dark gauge boson ($m_{Z'}$), the mass of the heavier sterile (m_h), the relative mass splitting (Δ), the mixing between muon neutrino and ν_h ($|U_{\mu 5}|^2$), the kinetic mixing between SM photon and dark gauge boson (ϵ) and the decay length of the heavy sterile ($c\tau_h$). To highlight how sensitive it is to viable solutions of the MiniBooNE anomaly, we restrict ourselves here to a few representative model points. Figure 5 shows the 95% CL exclusion sensitivity of this analysis to a set of 14 model parameter slices relevant for the MiniBooNE anomaly, assuming that we observe data consistent with background only.

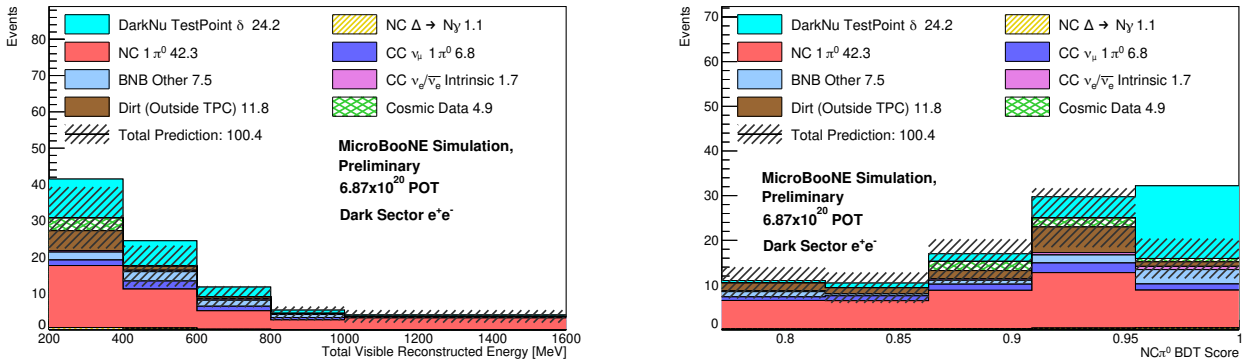

(a) Reconstructed visible energy of e^+e^- pair *(b) Neutral-current π^0 BDT score*

Figure 3: *The final predicted distributions for the e^+e^- selection from MicroBooNE Runs 1–3, corresponding to a 6.87×10^{20} POT exposure. This figures shows the total reconstructed visible energy of the e^+e^- pair (a) as well as the neutral-current π^0 BDT score (b), an important variable for rejecting backgrounds. Shown stacked on top of the backgrounds is a representative parameter point for the dark sector e^+e^- model, chosen to be on the edge of our expected sensitivity achievable at MicroBooNE. This test point consists of an 800 MeV Z', with two sterile neutrinos of 210 and 107 MeV respectively. We note that this representative point predicts a smaller rate of events in MiniBooNE compared to the observed anomaly. In general, model points that accurately match the rate of the anomaly in MiniBooNE predict $\mathcal{O}(100)$ e^+e^- events in MicroBooNE for this selection. This is primarily due to the coherent upscattering cross-section scaling proportional to neutron number squared, N^2, and moving from Mineral Oil ($N = 6$) to Argon ($N = 22$) targets*

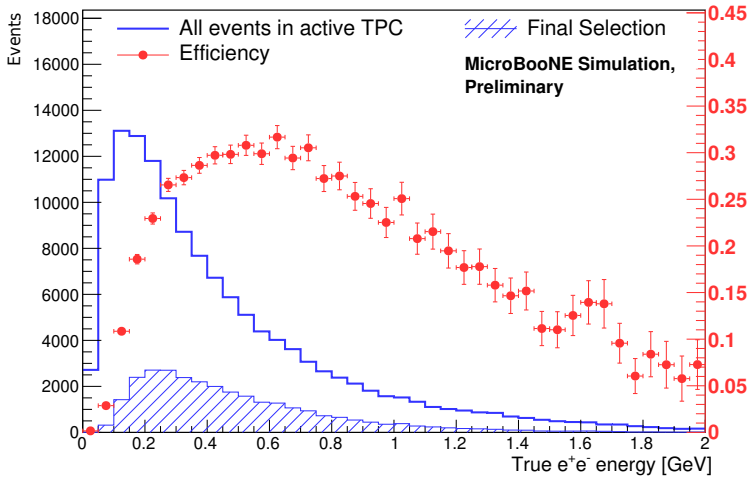

Figure 4: *Efficiency of selecting dark-sector e^+e^- pairs in the Pandora multi-topology based analysis, as a function of true e^+e^- energy. Efficiencies vary from around 18% at low energies such as 200 MeV to a peak of 30% at 600 MeV. This highlights the considerable improvement relative to the first generation photon LEE searches at MicroBooNE [4] whose efficiencies varied from 4% to 16% in the same range. The sample used in this study was constructed from a cocktail of four separate signal simulation monte-carlo files, varying the sterile mass and including both light and heavy Z' masses to best cover the parameter space of interest. The efficiency presented here is averaged over the e^+e^- opening angle and angle the pair makes with respect to the incoming neutrino beam.*

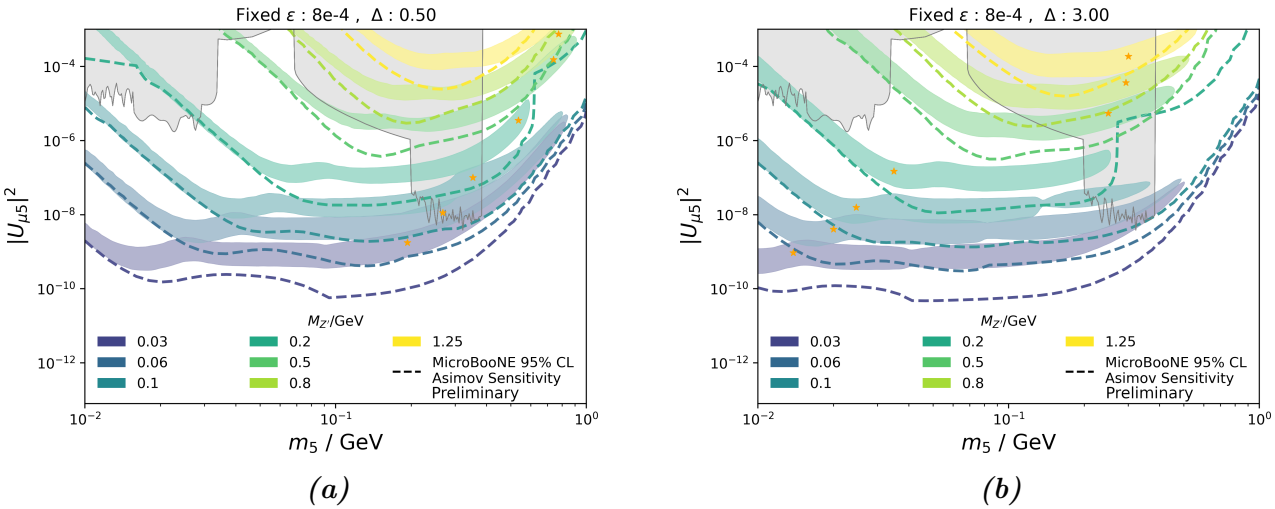

(a) *(b)*

Figure 5: *The 95% CL exclusion limit sensitivities assuming Asimov data and Wilks Theorem for 2 degrees of freedom (i.e. one separate exclusion per Δ and $m_{Z'}$ mass point). Each color represents a separate value of the dark gauge boson mass, and each MicroBooNE exclusion line excludes all above it. The allowed regions for MiniBooNE are taken from the phenomenological paper [1], and are at the 3σ level, with each gold star showing that particular masses best fit value. Left is for a smaller relative mass splittings between dark sector sterile neutrinos $\Delta = 0.5$ (a), and right for a larger $\Delta = 3.0$ (b). In all cases, MicroBooNE's sensitivity well covers the MiniBooNE best fit point, and excludes the majority of the 3σ allowed regions.*

As with the majority of photon and e^+e^- BSM signals, by far the dominant SM background in LArTPC detectors such as MicroBooNE is due to neutral current (NC) π^0 production, in which one of the subsequent daughter photons of the π^0 decay is not reconstructed. This can be due to the photon leaving the detector before pair conversion, or due to a reconstruction failure such as the photon being too low energy to successfully reconstruct at a high efficiency. Additionally, π^0's produced in the dirt surrounding the detector can result in one daughter photon scattering inside the TPC and one remaining outside and undetected, leading to a similar background. In order to ensure that these backgrounds are well modeled before looking at the signal region a series of sidebands were unblinded, insensitive to the BSM e^+e^- signal being searched for, but rich in a variety of SM backgrounds. Two of such sidebands are shown in Fig. 6 highlighting that these backgrounds are well modeled within our assigned systematic uncertainties. Both of these sidebands contain events consistent with the same three primary signal typologies we are searching for, 1s0t, 1s1t and 2s0t.

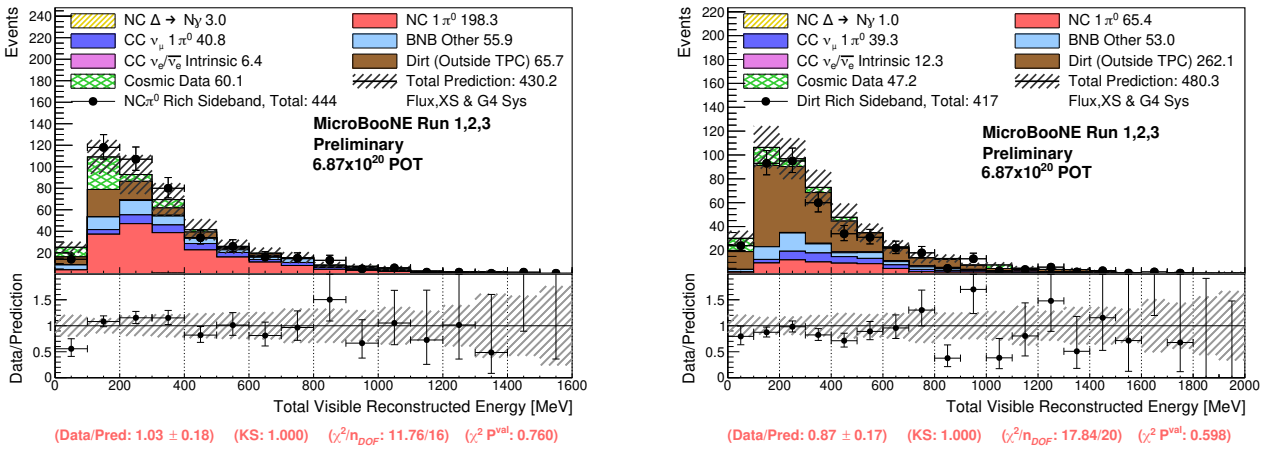

(a) *(b)*

Figure 6: *Validation sidebands with a focus on (a) NC π^0 backgrounds and (b) Dirt (Out-of-TPC) rich backgrounds. In both cases the data agrees well with our predicted simulation within our assigned systematic uncertainties in both these and all other variables studied.*

3 A focused light Z' dark sector search

Alongside the broader search for these dark sector models, a focused search for anomalous e^+e^- pairs utilizing the high-efficiency Wire-Cell reconstruction framework is also taking place at MicroBooNE. This specific model was first proposed in [14] as an explanation for the MiniBooNE anomaly and utilizes a dark gauge boson that is very light ($m_{Z'} << m_h$) relative to the sterile neutrino, resulting in both extremely prompt decays of the heavy neutrino after production by upscattering ($c\tau < 1$)mm and more overlapping e^+e^- pairs. This analysis is built from the original MicroBooNE inclusive electron low-energy excess search [3], with additional information tailored to target photon and e^+e^- like backgrounds. A specialized BDT is trained to select these dark sector e^+e^- events and reject SM backgrounds, with the resulting selection being defined as all events in which the BDT score is > 0.9. The final efficiency averaged over all model points for selecting true e^+e^- pairs for this BDT cut is shown in Fig. 7, with values ranging from 16% to 46% across all $m_{Z'}$ and m_h mass points studied, with majority being in the high efficiency 30–40% range.

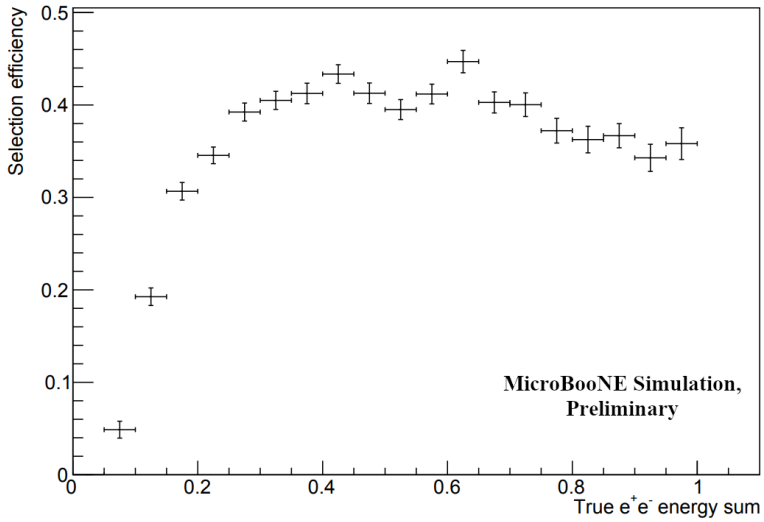

Figure 7: *The efficiency of the light gauge boson selection as a function of the true electron positron pair, with values peaking at 40% above 300 MeV. This is averaged over the opening angle of the e^+e^- pair and angle the pair makes with respect to the incoming neutrino beam.*

This analysis is extremely sensitive to the class of light Z' masses that were used to explain the MiniBooNE anomaly in [14]. In this reference, only the benchmark 30 MeV Z' model point has a published region of phase space that fits best to MiniBooNE. This region of interest is shown in Fig. 8 alongside the 95% CLs sensitivity of this focused MicroBooNE analysis. The 95% CLs sensitivity covers completely the MiniBooNE allowed 3σ region. We note that the prior bounds from CHARM and Minerva are not dedicated experimental searches, but reinterpretations of existing searches.

A variety of sidebands have been studied for this analysis also, focusing again on validating backgrounds and the tools developed to select the exotic e^+e^- pairs. In particular we highlight in one important sideband in Fig. 9, that is close to the signal region (BDT score between 0.6 and 0.7) and whose events have no evidence for any proton activity. We note that we do not expect MiniBooNE-scale BSM signals to produce visible e^+e^- events in this samples. We see good agreement in this sideband with respect to the expected backgrounds, within our assigned uncertainty, for a wide variety of kinematic and calorimetric variables studied.

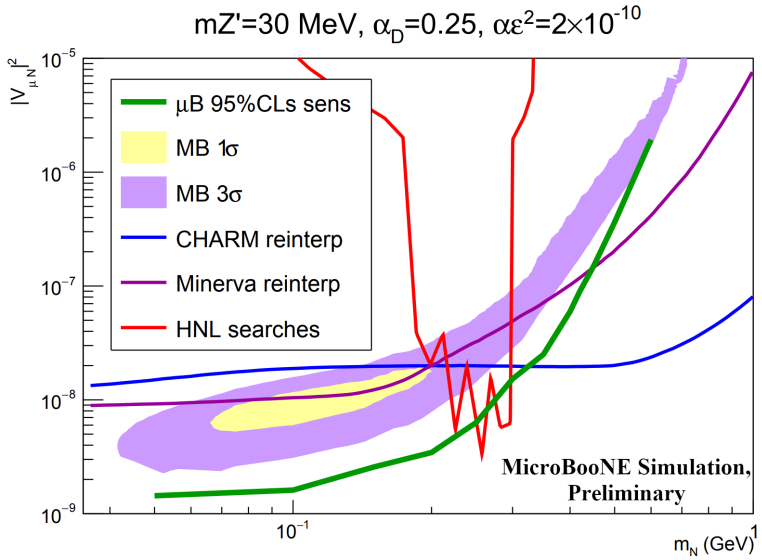

Figure 8: *Representative 95% CLs sensitivity of this MicroBooNE analysis to a specific model parameter point evaluated for a Dirac dark neutrino, with* $m_{Z'} = 30\,MeV$, $\alpha_D = 0.25$, $\epsilon^2\alpha_{EM} = 2 \times 10^{-10}$, $|U_{e4}|^2 = |U_{\tau 4}|^2 = 10^{-10}$. *MiniBooNE allowed region taken from [14]. Shown also are the indirect (reinterpretation) bounds from CHARM and Minerva taken from [11].*

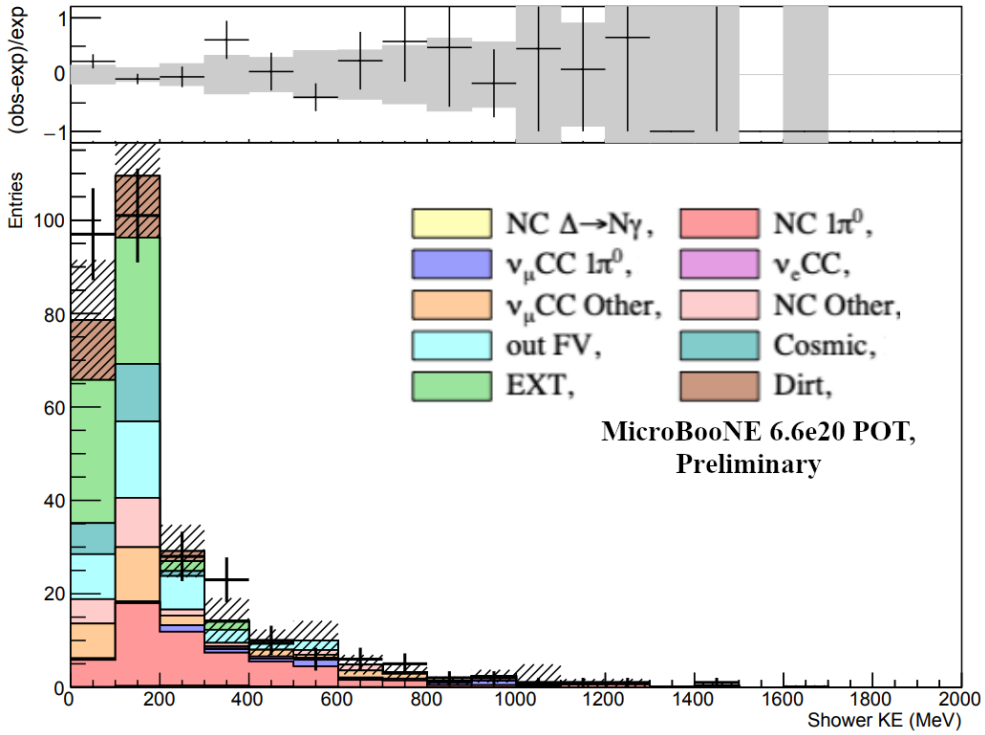

(a)

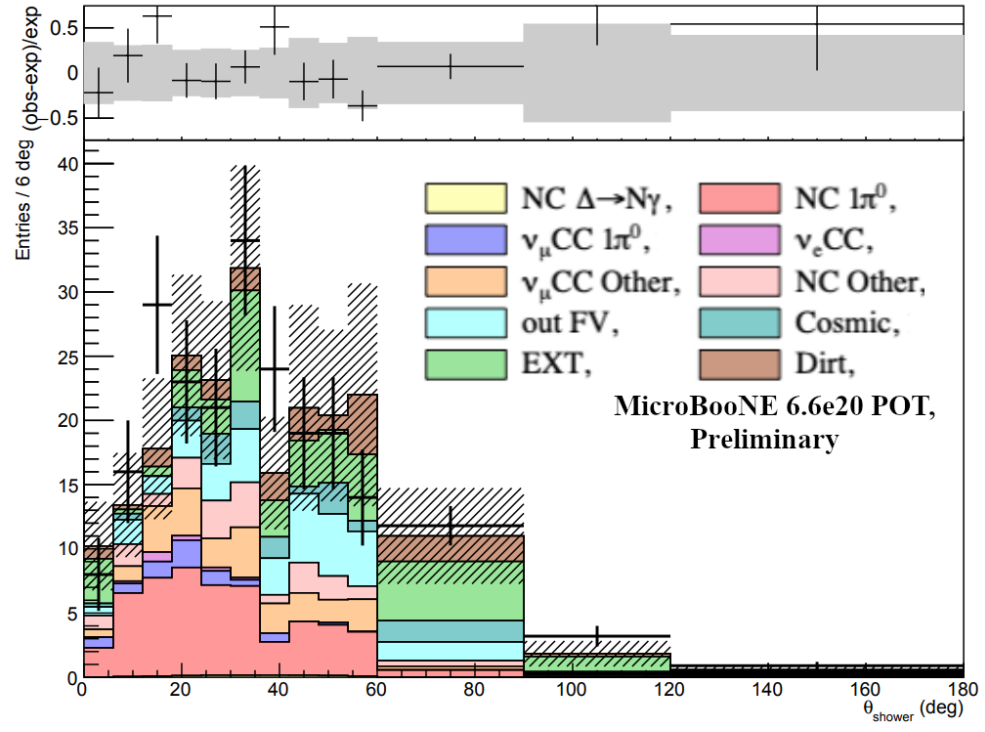

(b)

Figure 9: *Reconstructed shower energy (a) and reconstructed angle of shower with respect to the neutrino beam (b) of the signal-adjacent sideband sample, showing good data to Monte-Carlo predictions and giving confidence in our background predictions. Note that we do not expect MiniBooNE-scale BSM signals to produce any appreciable numbers of e^+e^- events in this sample. This is using 6.6×10^{20} POT from MicroBooNE's first three run periods.*

4 Conclusions

This note briefly describes the selections, efficiencies and sensitivities of two ongoing searches in the BNB at MicroBooNE for dark-sector induced e^+e^- anomalous signals. Showing substantial improvements in efficiency relative to the first generation MicroBooNE photon-like searches, the sensitivities of the analyses cover not only the regions of interest consistent with a possible explanation of the long standing MiniBooNE analysis, but probe a wider region of never before explored dark sector parameter space. Both analyses have been validated on a small sample of 5×10^{19} POT open data and an extensive suite of sideband studies, and are at the cusp of unblinding data corresponding to the first three run periods of MicroBooNE. With this data, these analyses will be able to confirm or reject almost all hypotheses that the MiniBooNE low energy excess is due to this class of upscattering dark sector models, and open the door to further dark sector searches at MicroBooNE and beyond.

References

[1] A. M. Abdullahi, J. Hoefken Zink, M. Hostert, D. Massaro, and S. Pascoli. A panorama of new-physics explanations to the MiniBooNE excess. arXiv:2308.02543 (2023).

[2] A. M. Abdullahi, J. Hoefken Zink, M. Hostert, D. Massaro, and S. Pascoli. DarkNews: A Python-based event generator for heavy neutral lepton production in neutrino-nucleus scattering. *Comput. Phys. Commun.*, 297:109075, 2024.

[3] P. Abratenko et al. Search for an anomalous excess of inclusive charged-current ν_e interactions in the MicroBooNE experiment using Wire-Cell reconstruction. *Phys. Rev. D*, 105(11):112005, 2022.

[4] P. Abratenko et al. Search for Neutrino-Induced Neutral-Current Δ Radiative Decay in MicroBooNE and a First Test of the MiniBooNE Low Energy Excess under a Single-Photon Hypothesis. *Phys. Rev. Lett.*, 128:111801, 2022.

[5] P. Abratenko et al. Wire-cell 3D pattern recognition techniques for neutrino event reconstruction in large LArTPCs: algorithm description and quantitative evaluation with MicroBooNE simulation. *JINST*, 17(01):P01037, 2022.

[6] R. Acciarri et al. Design and Construction of the MicroBooNE Detector. *JINST*, 12(02):P02017, 2017.

[7] R. Acciarri et al. The Pandora multi-algorithm approach to automated pattern recognition of cosmic-ray muon and neutrino events in the MicroBooNE detector. *The European Physical Journal C*, 78(1):82, 2018.

[8] M. A. Acero et al. White Paper on Light Sterile Neutrino Searches and Related Phenomenology. *arXiv:2203.07323 hep-ex*, 3 2022.

[9] A. A. Aguilar-Arevalo et al. Significant Excess of ElectronLike Events in the MiniBooNE Short-Baseline Neutrino Experiment. *Phys. Rev. Lett.*, 121(22):221801, 2018.

[10] C. Andreopoulos et al. The GENIE Neutrino Monte Carlo Generator. *Nucl. Instrum. Meth. A*, 614:87–104, 2010.

[11] C. A. Argüelles, M. Hostert, and Y.-D. Tsai. Testing New Physics Explanations of the MiniBooNE Anomaly at Neutrino Scattering Experiments. *Phys. Rev. Lett.*, 123(26):261801, 2019.

[12] P. Ballett, M. Hostert, and S. Pascoli. Dark Neutrinos and a Three Portal Connection to the Standard Model. *Phys. Rev. D*, 101(11):115025, 2020.

[13] P. Ballett, S. Pascoli, and M. Ross-Lonergan. U(1)' mediated decays of heavy sterile neutrinos in MiniBooNE. *Phys. Rev. D*, 99:071701, 2019.

[14] E. Bertuzzo, S. Jana, P. A. N. Machado, and R. Zukanovich Funchal. Dark Neutrino Portal to Explain MiniBooNE excess. *Phys. Rev. Lett.*, 121(24):241801, 2018.